Journal of Experimental and Theoretical Physics, Vol. 101, No. 6, 2005, pp. 1098–1105.
From Zhurnal Éksperimental'noĭ i Teoreticheskoĭ Fiziki, Vol. 128, No. 6, 2005, pp. 1252–1259.
Original English Text Copyright © 2005 by Kharlamova, Ovchinnikov, Balaev, Thomas, Lyubutin, Gavriliuk.

ORDER, DISORDER, AND PHASE TRANSITIONS IN CONDENSED SYSTEMS

Spin Reorientation Effects in $GdFe_3(BO_3)_4$ Induced by Applied Field and Temperature¶

S. A. Kharlamova[a], S. G. Ovchinnikov[a], A. D. Balaev[a], M. F. Thomas[b], I. S. Lyubutin[c], and A. G. Gavriliuk[c]

[a]*Kirensky Institute of Physics, Siberian Branch of Russian Academy of Sciences, Krasnoyarsk, 660036 Russia*
[b]*University of Liverpool, L69 3BX, Liverpool, Great Britain*
[c]*Institute of Crystallography, Moscow, 119333 Russia*
e-mail: lyubutin@ns.crys.ras.ru
Received May 16, 2005

Abstract—Magnetic properties of $GdFe_3(BO_3)_4$ single crystals were investigated by ^{57}Fe-Mössbauer spectroscopy and static magnetic measurements. In the ground state, the $GdFe_3(BO_3)_4$ crystal is an easy-axis compensated antiferromagnet, but the easy axis of iron moments does not coincide with the crystal C_3 axis, deviating from it by about 20°. The spontaneous and field-induced spin reorientation effects were observed and studied in detail. The specific directions of iron magnetic moments were determined for different temperatures and applied fields. Large values of the angle between the Fe^{3+} magnetic moments and the C_3 axis in the easy-axis phase and between Fe^{3+} moments and the a_2 axis in the easy-plane phase reveal the tilted antiferromagnetic structure. © *2005 Pleiades Publishing, Inc.*

1. INTRODUCTION

The crystal $GdFe_3(BO_3)_4$ belongs to the family of rare-earth borates $RM_3(BO_3)_4$, where R is a rare-earth element and M = Al, Ga, Fe, Sc, and has a trigonal symmetry with the space group $R32$ (D_{3h}^7) [1, 2]. These materials first attracted great interest because of promising nonlinear and laser properties [3–5]. Quite recently, a magnetoelectrical effect was found in $GdFe_3(BO_3)_4$, which suggests that this crystal be considered as a new multiferroic material [6].

The crystal structure of $GdFe_3(BO_3)_4$ can be represented by layers oriented perpendicular to the C_3 axis and consisting of trigonal GdO_6 prisms and smaller FeO_6 octahedrons [2]. The FeO_6 octahedrons are connected by edges and create one-dimensional spiral chains directed along the threefold C_3 axis (Fig. 1). The shortest Fe–Fe interionic distance in chains is about 3.155 Å and that between chains is 4.361 Å, whereas the shortest Fe–Gd distance is 3.746 Å [2]. Exchange interaction between iron ions from different chains is weak and the chains are mutually independent.

Magnetization and magnetic susceptibility measurements have shown that $GdFe_3(BO_3)_4$ is an antiferromagnet with the Néel temperature T_N = 38 K and its magnetic moments are directed along the crystal C_3 axis [7, 8]. It was suggested that magnetic ordering relates to Fe ions, whereas Gd ions are paramagnetic at least down to liquid-helium temperature [7]. However, recent studies of antiferromagnetic resonance [9] indicated that a possible magnetic ordering of the Gd ions at low temperatures can play an essential role in magnetic anisotropy of the crystal and influence the direction of the iron magnetic moment. The competition of the magnetic anisotropy and indirect coupling between Fe–O–Fe chains via Gd^{3+} results in a range of interesting magnetic behavior and, in particular, may be responsible for the spin-reorientation effect observed in [7, 10]. In addition to the low-temperature magnetic transitions, a structural phase transition was observed at 156 K [11]; two electronic and structural phase transitions induced by high pressures at P = 26 GPa and P = 42 GPa and at room temperature were found by optical and X-ray studies [12].

Calculations predicted [6] that the electric polarization and the magnetostriction appearing in $GdFe_3(BO_3)_4$ at low temperatures (the magnetoelectrical effects) are the result of changes in magnetic symmetry during the spin-reorientation transition induced by an applied magnetic field.

Thus, detailed information about distinctive features of the spin-reorientation effect in $GdFe_3(BO_3)_4$ is extremely important for understanding the low-temperature properties and the nature of the magnetoelectrical effect in this material.

In the present paper, in addition to static magnetic measurements, ^{57}Fe-Mössbauer spectroscopy studies were carried out at different temperatures and in an applied magnetic field with single-crystalline samples

¶ The text was submitted by the authors in English.

of $GdFe_3(BO_3)_4$. The temperature and magnetic-field induced spin-reorientation transitions of the Fe^{3+} magnetic moments were found and investigated on both macroscopic and microscopic scales.

2. EXPERIMENTAL

High-quality crystals of $GdFe_3(BO_3)_4$ were grown by the flux method [7]. The crystals were transparent and had green color. The unit cell parameters are a = 9.5491(6) Å and c = 7.5741(5) Å. For the Mössbauer measurements, a platelet with dimensions of 8×5 mm^2 and thickness of 0.3 mm was cut from the bulk single crystal. The C_3 axis was in the plane of the platelet.

Static measurements of magnetization and magnetic susceptibility were carried out using a vibrating-sample magnetometer with a superconducting magnet in the temperature range 4.2–300 K. An external magnetic field up to 7.5 T was applied parallel and perpendicular to the C_3 axis.

The ^{57}Fe-Mössbauer spectra were recorded in transmission geometry with standard spectrometers operating in the constant acceleration regime. Gamma-ray sources of ^{57}Co(Cr) and ^{57}Co(Rh) were used. Three sets of Mössbauer experiments have been carried out with the single-crystalline sample.

In the first set, the Mössbauer spectra were recorded at temperatures of 5, 20, 40, and 300 K in zero applied magnetic field and with the propagation vector $\mathbf{k}_\gamma$ of the Mössbauer gamma rays directed perpendicular to the crystal platelet.

In the second set, the spectra were recorded at 4.2 K in external magnetic fields H = 0, 0.3, and 1.0 T applied in the plane of crystal platelet perpendicular to the direction of the sample C_3 axis. The propagation vector of the Mössbauer gamma rays was directed perpendicular to the crystal platelet; i.e., the C_3 axis, the applied field, and the gamma rays were all mutually perpendicular.

In the third set, the spectra were recorded at 4.2 K in external magnetic fields H = 0, 2.0, and 4.0 T applied in the plane of the crystal platelet, but parallel to the C_3 axis.

3. RESULTS AND DISCUSSIONS

3.1. Summary Results of the Static Magnetic Measurements

Temperature dependences of the direct χ and reciprocal $1/\chi$ magnetic susceptibility with the applied field 0.1 T are shown in Fig. 2. Two anomalies are observed when the field **H** is applied parallel and perpendicular to the crystal C_3 axis. At 38 K, the deviation of $\chi^{-1}(T)$ from the linear law implies a transition from the paramagnetic to an antiferromagnetic state, and the sharp anomaly near 10 K indicates a change of the magnetic structure of $GdFe_3(BO_3)_4$.

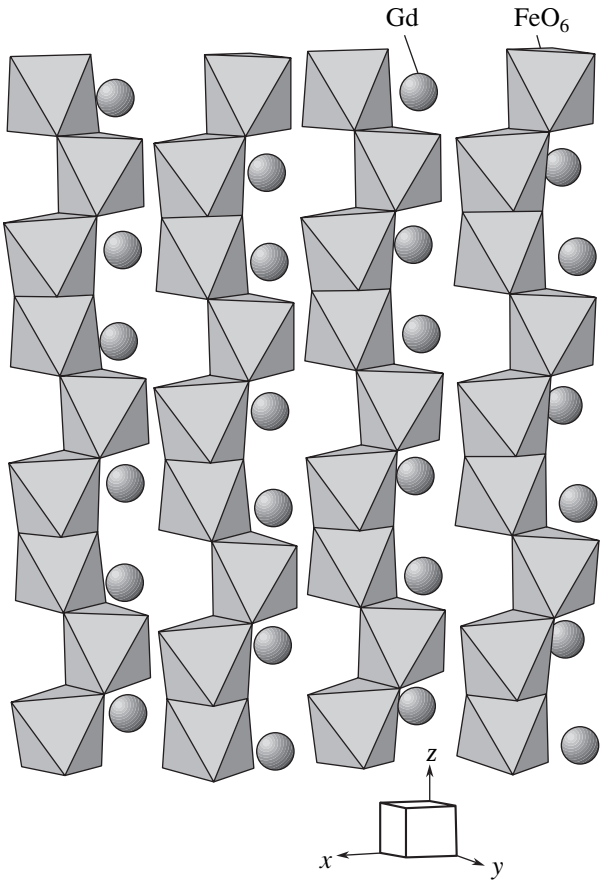

Fig. 1. A fragment of the $GdFe_3(BO_3)_4$ crystal structure showing the oxygen octahedra (the iron ions sites) generating helical chains along the C_3 axis [2].

The field dependences of the magnetization $M(H)$ at 4.2 K are shown in Fig. 3. When the magnetic field is perpendicular to the C_3 axis, the $M(H)$ dependence is almost linear in the range of $0 < H < 3$ T, and magnetization vanishes at zero field (see Fig. 3, inset a). This behavior indicates that the ground state of $GdFe_3(BO_3)_4$ is a compensated antiferromagnet. When **H** is parallel to the C_3 axis, a sharp increase in magnetization was observed at the critical field $H_{reor} \approx 0.6$ T. At this point, M reaches the value typical of that for the case when **H** is perpendicular to the C_3 axis (see Fig. 3). This indicates that a magnetic moment reorientation from the C_3 axis to the plane perpendicular to the C_3 axis occurs. With a further increase in field, an additional anomaly is observed near $H \approx 3.1$ T (see inset b to Fig. 3), which can be attributed to the appearance of the spontaneous magnetic moment induced in the basal plane.

We found that the critical field of reorientation, H_{reor}, decreases with increasing temperature. Figure 4 presents tentative magnetic phase diagrams showing

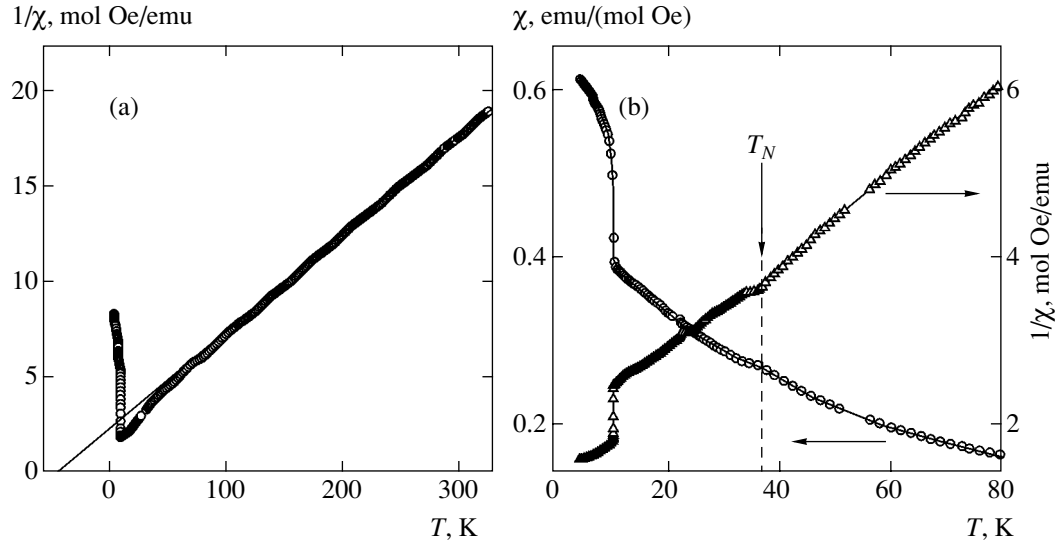

Fig. 2. Temperature dependences of the reciprocal $1/\chi$ and direct χ magnetic susceptibility in the magnetic field $H = 0.1$ T applied parallel (a) and perpendicular (b) to the C_3 axis.

the values of critical fields H_{reor} and corresponding temperatures at which the magnetic moment reorientation occurs when the external field is parallel and perpendicular to the C_3 axis. Along with our data of the static magnetic measurements, the results in [6] from electric polarization and magnetostriction measurements and the results in [9] from the antiferromagnetic resonance measurements are also included in the phase diagram of Fig. 4. One can see that different methods give good agreement for the critical field and its dependence on temperature. The dashed line is a visual guide that separates the two magnetic phases at the reorientation transition from the easy-axis state to the easy-plane state.

3.2. ^{57}Fe-Mössbauer Spectroscopy Results

1. The ^{57}Fe-Mössbauer spectra of the first set of measurements in zero applied field are shown in Fig. 5. At temperatures of 5 and 20 K, the magnetic hyperfine splitting of resonance lines indicates a magnetic ordering of the Fe ions. A single six-line spectrum with a rather narrow linewidth shows that all iron ions occupy equivalent crystal sites, even though the antiferromagnetic ordering implies the existence of at least two iron magnetic sublattices. The magnetic hyperfine field H_{hf} at a ^{57}Fe nuclei and the isomer shift (IS) values are typical of the high-spin Fe^{3+} state (see table). At 40 and 300 K, the spectra show a slightly asymmetric quadrupole doublet characteristic of the iron paramagnetic state. The line broadening at 40 K (see table) is apparently related to a trace of magnetic ordering because the Néel temperature is very close to this temperature. The decrease of the IS value with increasing temperature from 5 to 300 K (see table) is related to the second-order Doppler shift. However, the evident increase of the IS at the transition from the antiferromagnetic to paramagnetic state is an indication of some changes in the chemical bonds and/or the electronic state of the iron ions, which can be related to crystal distortion at the magnetic transition [6].

Special attention should be paid to the behavior of the line intensities in the spectra at 5 and 20 K (see Fig. 5). In general, the line intensities are defined by the probabilities of the Mössbauer transitions between nuclear sublevels and depend on the angle θ between the propagation vector $\mathbf{k}_\gamma$ of the gamma rays and the direction of magnetic hyperfine field H_{hf} at the ^{57}Fe nuclei, which should coincide with the iron magnetic

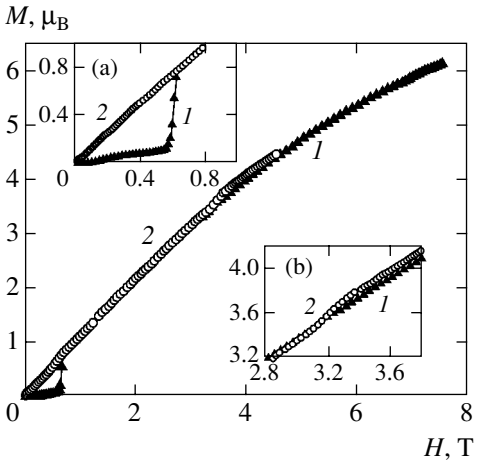

Fig. 3. The field dependences of $GdFe_3(BO_3)_4$ magnetization at 4.2 K in the magnetic field applied parallel (*1*) and perpendicular (*2*) to the C_3 axis. Insets (a) and (b) show the observed anomalies on an enlarged scale.

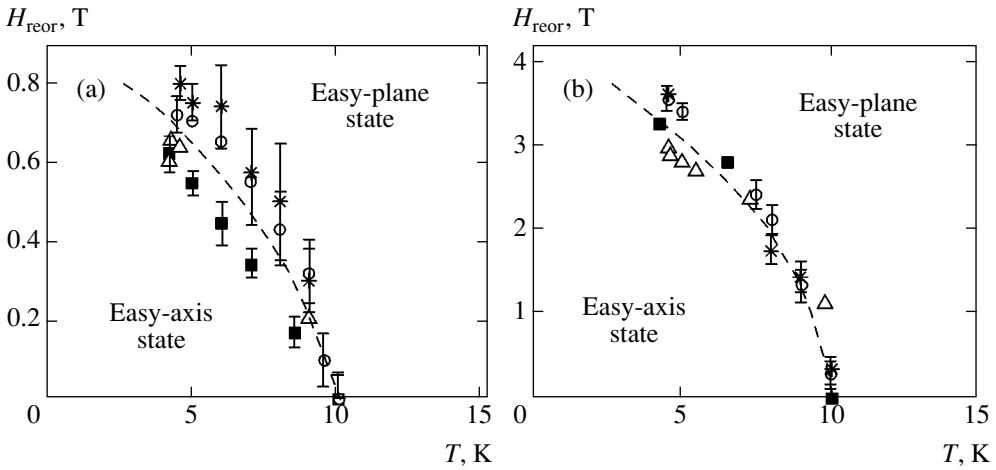

Fig. 4. The tentative magnetic phase diagram for $GdFe_3(BO_3)_4$ showing the values of critical fields H_{reor} and corresponding temperatures at which the iron moments reorientation occurs when the external field is parallel (a) and perpendicular (b) to the C_3 axis. Along with our data (■), the data from the electric polarization (∗) and magnetostriction (○) measurements [6] and the data from the antiferromagnetic resonance measurements (▲) [9] are shown. In both (a) and (b), the dashed line is a visual guide for the eye and separates the two magnetic phases at the reorientation transition from the easy-axis state to the easy-plane state.

moment. For a thin absorber, the intensities I_i (i = 1, 2,…, 6) of a six-line Zeeman spectrum are in a ratio of

$$I_1 : I_2 : I_3 = I_6 : I_5 : I_4 = 3 : \alpha : 1,$$

where

$$\alpha = \frac{4\sin^2\theta}{1 + \cos^2\theta}. \quad (1)$$

In a powder sample, a spherical average of the angle distribution ($\cos^2\theta = 1/3$, $\sin^2\theta = 2/3$) gives

$$I_1 : I_2 : I_3 = I_6 : I_5 : I_4 = 3 : 2 : 1.$$

At a random orientation of a single crystal, the θ value can be obtained from

$$\cos^2\theta = 1 - \frac{2(I_2 + I_1)}{\frac{6}{\sum_{i=1} I_i}}. \quad (2)$$

Thus, it follows from the spectra in Fig. 5 that at temperatures between 5 and 20 K, the iron magnetic moment in $GdFe_3(BO_3)_4$ changes its orientation. From the line intensity ratio in Eq. (2), we found that the iron moments make the angle $\theta = 68 \pm 3°$ with the $\mathbf{k}_\gamma$ vector at 5 K, and this angle changes at 20 K. The low-temperature value of θ indicates that the iron magnetic moments are not in the crystal plane but deviate from it by the angle $\beta = 90° - 68° = 22 \pm 3°$.

Additional information on the direction of the iron magnetic moment can be obtained from the behavior of the quadrupole shift in the Zeeman spectrum below the

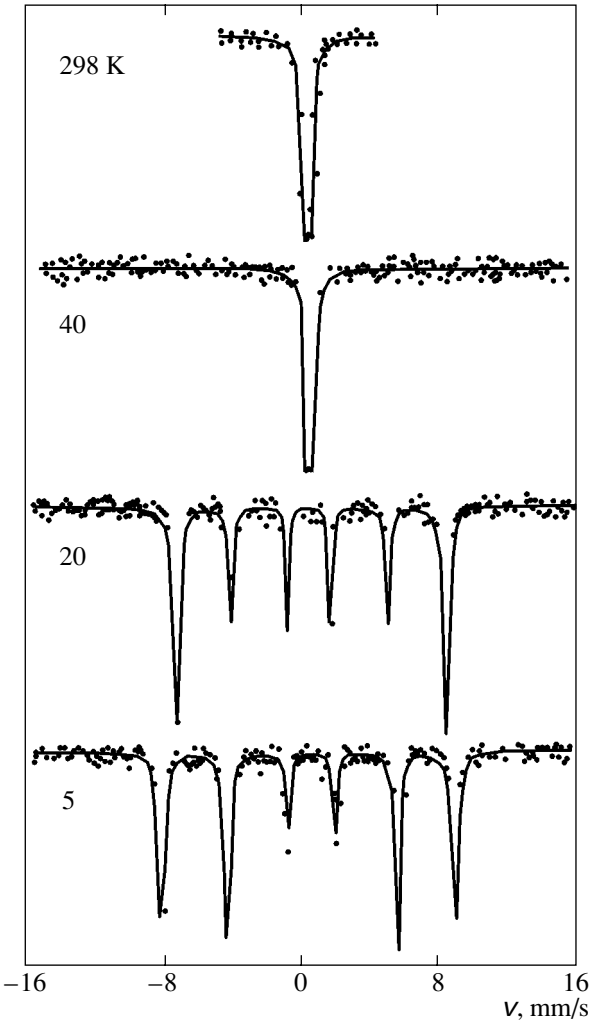

Fig. 5. The ^{57}Fe-Mössbauer spectra of the $GdFe_3(BO_3)_4$ single crystal recorded at temperatures 5, 20, 40, and 298 K in zero applied magnetic field.

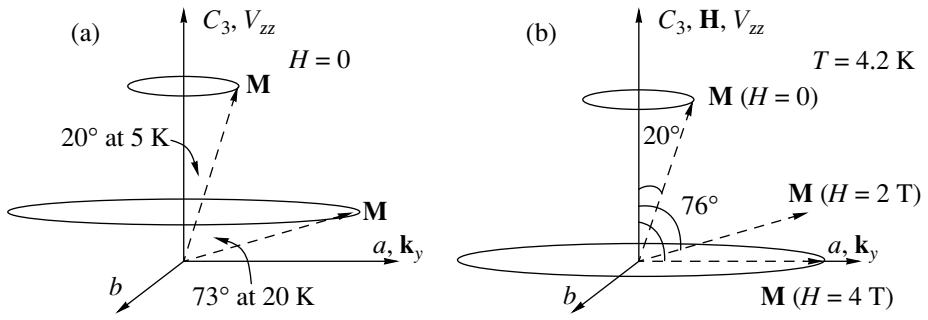

Fig. 6. Effects of reorientation of the Fe magnetic moments in $GdFe_3(BO_3)_4$ deduced from the Mössbauer measurements under the assumption that the hyperfine magnetic field $\mathbf{H}_{hf}$ at the ^{57}Fe nuclei coincides with the iron magnetic moment **M**. Mutual directions of the crystal C_3 axis, the main axis of the electric-field gradient V_{zz}, the applied magnetic field **H**, the gamma-ray propagation vector $\mathbf{k}_\gamma$, and the iron magnetic moments **M** are shown for different temperatures (a) and applied magnetic fields (b). In the case where the antiferromagnetic iron sublattices are collinear, the arrow **M** in (a) and (b) represents the iron antiferromagnetic vector **L**.

Néel temperature. When the magnetic hyperfine interaction is much stronger than the electric quadrupole interaction, the quadrupole shift of the spectral lines observed below the Néel temperature, $(e^2qQ)_{obs}$, and the true quadrupole splitting e^2qQ (which can be obtained above the Néel temperature) are related by

$$(e^2qQ)_{obs} \approx e^2qQ\frac{3\cos^2\varphi - 1}{2}. \qquad (3)$$

Here, Q is the nuclear quadrupole moment and φ is the angle between the direction of the iron magnetic moment and the main axis of electric-field gradient $eq = V_{zz} = \partial^2V/\partial z^2$ [13]. We neglect the asymmetry parameter $\eta = (V_{xx} - V_{yy})/V_{zz}$ in Eq. (3) because of the local C_3 symmetry.

Thus, the angle dependence of $(e^2qQ)_{obs}$ can be used to find the direction of iron moment relative to the crystal axes if the main axis of the electric-field gradient V_{zz} is known. Due to crystallographic reasons, we suppose that in the paramagnetic state of $GdFe_3(BO_3)_4$, the sign of the quadrupole interaction is negative. From the quadrupole shift at $T = 5$ K (Fig. 5), we found the angle φ between Fe moments and V_{zz} direction to be $18 \pm 2°$. It

Hyperfine parameters of the ^{57}Fe-Mössbauer spectra of the $GdFe_3(BO_3)_4$ single crystal: H_{hf} is the hyperfine magnetic field at a ^{57}Fe nuclei, IS is the isomer shift relative to α-Fe at room temperature, QS is the quadrupole shift (splitting), Γ is the linewidth, H is the applied magnetic field, and φ is the angle between the direction of iron magnetic moments and the main axis of electric-field gradient V_{zz}

T, K	H, T	H_{hf}, kOe	IS, mm/s	QS, mm/s	Γ, mm/s	φ
5	0	526.5(2)	0.503(3)	−0.247(6)	0.365(8)	18.3 ± 2.0°
20	0	481.7(2)	0.504(2)	+0.107(4)	0.333(6)	72.8 ± 2.0°
40	0	~0	0.554(2)	0.290(2)	0.431(3)	–
300	0	0	0.390(2)	0.292(2)	0.300(3)	–
External field **H** is perpendicular to the C_3 axis						
4.2	0	527.7(6)	0.485(7)	−0.269(15)	0.39(2)	12 ± 8°
4.2	0.3	527.7(5)	0.497(6)	−0.270(15)	0.37(2)	12 ± 8°
4.2	1.0	527.2(4)	0.497(5)	−0.243(11)	0.38(2)	19.2 ± 2.0°
External field **H** is parallel to the C_3 axis						
4.2	0	527.8(4)	0.510(5)	−0.232(10)	0.380(13)	21.5 ± 2.0°
4.2	2.0	529.8(2)	0.500(4)	+0.120(7)	0.362(10)	76.2 ± 1.5°
4.2	4.0	529.4(2)	0.493(3)	+0.144(6)	0.349(8)	87.3 ± 1.5°

is significant that the angles $\beta = 22 \pm 3°$ and $\varphi = 18 \pm 2°$ agree within their uncertainties and indicate that V_{zz} coincides with the crystal C_3 axis. This suggests that the main axis of the electric-field gradient at an iron nuclei is directed along the local threefold axis of an oxygen octahedral (see Fig. 1). This also shows that at 5 K, the iron moments are not directed precisely along the C_3 axis, but rather at an angle of about 20°.

From the quadrupole shift, we derive an increase of the φ angle to $73 \pm 2°$ at 20 K. If there are no structural transitions between 5 and 20 K, the V_{zz} direction should remain along the C_3 axis. This means that at 20 K, the iron magnetic moments include the angle $73 \pm 2°$ with the C_3 axis (Fig. 6a) and deviate from the basal plane by about $18 \pm 2°$. The intensities of the second and fifth spectral lines also change (Fig. 5), supporting the rotation of the iron spins.

Thus, two independent Mössbauer spectra parameters, the line intensity and the quadrupole shift, indicate that the reorientation of iron magnetic moments occurs in $GdFe_3(BO_3)_4$ at temperatures between 5 and 20 K. In Fig. 6a, mutual directions of the crystal C_3 axis, the main axis of the electric-field gradient V_{zz}, the gamma-ray propagation vector $\mathbf{k}_\gamma$, and the iron magnetic moments **M** are shown for different temperatures under the assumption that the direction of the magnetic hyperfine field $\mathbf{H}_{hf}$ at ^{57}Fe nuclei coincides with the direction of the iron magnetic moments.

2. In the second setup of experiments, the $\mathbf{k}_\gamma$ vector, the C_3 axis, and the external magnetic field **H** were all mutually perpendicular. The spectra of this series recorded at 4.2 K are shown in Fig. 7a. The external fields of 0.3 and 1.0 T applied perpendicular to the crystal C_3 axis do not significantly change the hyperfine parameters at 4.2 K (see table). The iron magnetic sublattices do not lead to the absorption line split and the values of the magnetic hyperfine field H_{hf} are unchanged (see table). This correlates with the suggestion that **H** and $\mathbf{H}_{hf}$ are almost perpendicular. The areas of spectral lines 2 and 5 show that the fields $\mathbf{H}_{hf}$ (and the Fe moments) are not perpendicular to the gamma-ray beam but are at angles of about $\theta = 68 \pm 5°$ (at $H = 0$ and $H = 0.3$ T) and $\theta = 65 \pm 5°$ (at $H = 1.0$ T) to the $\mathbf{k}_\gamma$ vector. The values of the angle φ between the Fe moments and V_{zz} (i.e., the C_3 axis), estimated from the quadrupole shift, are the same for all H and close to the value estimated above at 5 K for zero applied field (i.e., φ is near 20°) within experimental error.

Thus, this series of experiments supports the conclusion derived in Section 3.2.1 that in the low-temperature phase of $GdFe_3(BO_3)_4$ near 4.2 K, the Fe moments deviate from the C_3 axis by an angle of about 20°.

3. The spectra of the third set of experiments with the external field applied along the C_3 axis are shown in Fig. 7b, and the hyperfine parameters are listed in the table. At a fixed temperature of 4.2 K, the changes in intensities of spectrum lines 2 and 5 clearly show the spin reorientation effect induced by the applied field. In the field of 4.0 T, all Fe magnetic moments line up

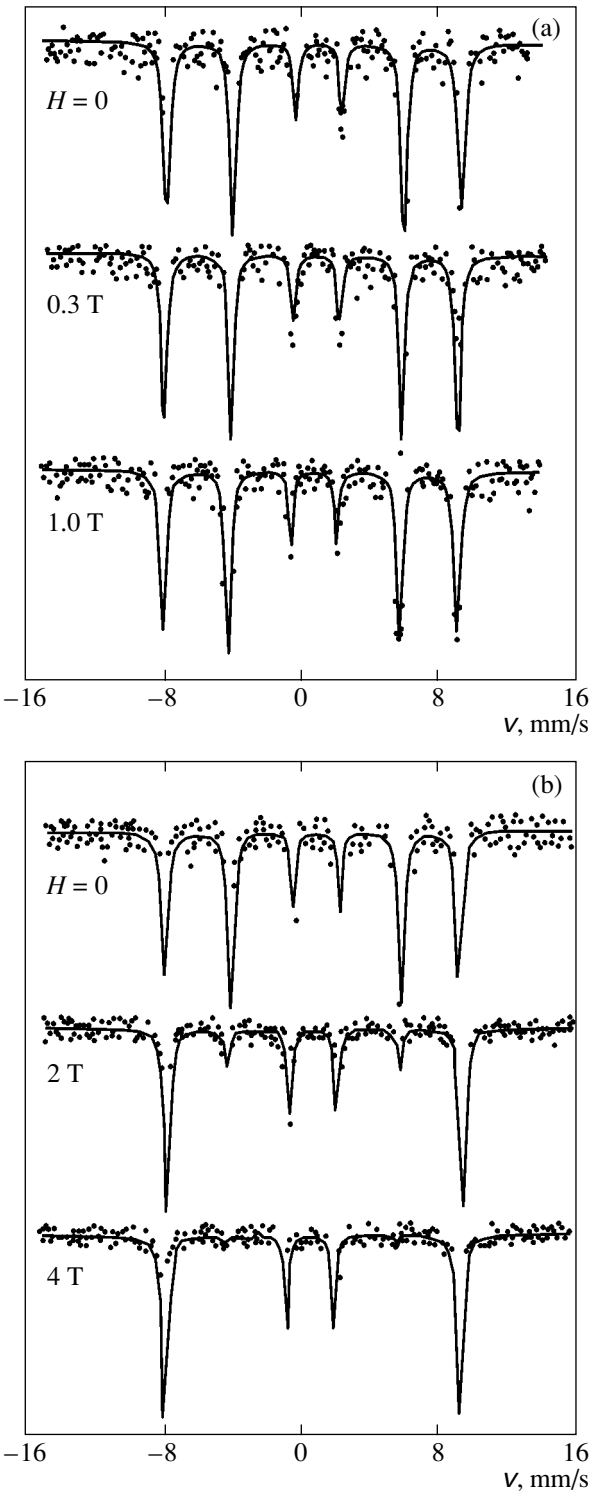

Fig. 7. ^{57}Fe-Mössbauer spectra of the $GdFe_3(BO_3)_4$ single crystal recorded at 4.2 K in external magnetic field applied perpendicular (a) and parallel (b) to the crystal C_3 axis.

along the $\mathbf{k}_\gamma$ vector ($\theta \approx 0$). This means that the angle β between the iron moments and the C_3 axis is near 90°. The behavior of the quadrupole shift supports this observation: the estimated angles φ are about 76.2 ± 1.5° at $H = 2$ T and 87.3 ± 1.5° at $H = 4$ T (see Fig. 6b). The agreement of the β and φ angle values at $H = 4$ T again supports the conclusion made in Section 3.2.1 that V_{zz} direction coincides with the crystal C_3 axis.

Thus, the external field applied along the C_3 axis rotates the iron spins in the (aC_3) plane of the crystal towards the basal plane (see Fig. 6b). At $H = 4$ T, the iron moments are oriented perpendicular to the C_3 axis and also perpendicular to the applied field.

It should be noted that if the antiferromagnetic iron sublattices are collinear, the arrow M in Fig. 6 represents the iron antiferromagnetic vector **L**.

In the basal plane of $GdFe_3(BO_3)_4$, there are three twofold a_2 axes at the angles 120° relative to each other. However, the Mössbauer experiment shows that in spite of the equivalence of the three a_2 axes, the iron moments in the basic plane are aligned completely along only one of the a_2 axes, just the one directed perpendicular to the crystal platelet. It seems that in a thin crystal platelet, the surface anisotropy plays an important role in the iron spin orientation.

In the case of collinear antiferromagnetic ordering of two Fe sublattices, the external field applied along the antiferromagnetic vector would increase ($\mathbf{H}_{tot} = \mathbf{H}_{hf} + \mathbf{H}$) or decrease ($\mathbf{H}_{tot} = \mathbf{H}_{hf} - \mathbf{H}$) the total field H_{tot} at iron nuclei in these sublattices. But the Mössbauer spectra in Fig. 7 show that the applied field does not split the absorption lines and only slightly modifies the H_{tot} value. Rotation of the iron spins normal to **H** with a negligible contribution of the $\mathbf{H}_{hf}$ projection onto **H** explains this behavior.

4. SUMMARY

From the two series of Mössbauer measurements on $GdFe_3(BO_3)_4$ single crystals, we have established that the main axis of the electric-field gradient, V_{zz}, is directed along the crystal C_3 axis.

Our phase diagram in Fig. 4 obtained from the magnetic static measurements shows good agreement with magnetic resonance [9] and electrical polarization and magnetostriction data [6]. The ^{57}Fe-Mössbauer spectroscopy data confirm the spin reorientation transition, first observed in $GdFe_3(BO_3)_4$ by the magnetic static measurements, and give new information on the specific orientation of the iron magnetic moments and the values of angles between the moments and crystal axes at different temperatures and applied fields. In the ground state at 4.2 K, the $GdFe_3(BO_3)_4$ crystal is an easy-axis compensated antiferromagnet. However, the easy axis of the iron moments deviates from the crystal C_3 axis by about 20°.

At about 10 K, the iron magnetic moments reorient spontaneously from the easy axis towards the basal plane. However, at 20 K, the moments are not entirely in the basal plane but deviate from it at about 18°. At 4.2 K, the external field of 1.0 T, applied perpendicular to the C_3 axis, does not influence the iron spins direction. This correlates with the magnetization behavior shown in inset *a* to Fig. 3. The field H applied along the C_3 axis gradually rotates iron moments in the (aC_3) plane toward the basal plane, and at $H = 4$ T, the moments are entirely in the plane. In the basic plane, the iron moments are directed along the crystal a_2 axis, which is perpendicular to the crystal platelet.

Thus, we have found that the magnetic structure of $GdFe_3(BO_3)_4$ is more complicated than it was suggested in [9]. The large values of the angle between the Fe^{3+} magnetic moments and the C_3 axis in the easy-axis phase and between the Fe^{3+} moments and the a_2 axis in the easy-plane phase reveal a tilted antiferromagnetic structure. The origin of this tilting is the competition of the two contributions to the magnetic anisotropy from the Fe^{3+} and Gd^{3+} sublattices. The decreasing of symmetry below the structural phase transition at $T = 156$ K and also below the Néel temperature $T_N = 38$ K [6] provides an additional contribution to the deviation of the magnetic moments from the crystallographic axes.

ACKNOWLEDGMENTS

We are grateful very much to S.N. Sul'yanov for the X-ray analysis of the crystal orientations. We thank A.K. Zvezdin and S.S. Krotov for fruitful discussions. We deeply appreciate the help of W. Sturhahn, who read the manuscript and made valuable comments. This work was supported by the Russian Foundation for Basic Research, project nos. 05-02-16142a, 03-02-16286a, and 04-02-16945a and by the program of the Russian Academy of Sciences "Strongly Correlated Electron Systems."

REFERENCES

1. J. A. Campá, C. Cascales, E. Gutiérrez-Puebla, *et al.*, Chem. Mater. **9**, 237 (1997).
2. N. I. Leonyuk and L. I. Leonyuk, Prog. Cryst. Growth Charact. **31**, 179 (1995); N. I. Leonyuk, Prog. Cryst. Growth Charact. **31**, 279 (1995).
3. D. Jaque, J. Alloys Compd. **323**–**324**, 204 (2001).
4. M. Huang, Y. Chen, X. Chen, *et al.*, Opt. Commun. **208**, 163 (2002).

5. X. Chen, Z. Luo, D. Jaque, *et al.*, J. Phys.: Condens. Matter **13**, 1171 (2001).
6. A. K. Zvezdin, S. S. Krotov, A. M. Kadomtseva, *et al.*, Pis'ma Zh. Éksp. Teor. Fiz. **81**, 335 (2005) [JETP Lett. **81**, 272 (2005)].
7. A. D. Balaev, L. N. Bezmaternykh, I. A. Gudim, *et al.*, J. Magn. Magn. Mater. C **258**–**259**, 532 (2003).
8. A. D. Balaev, L. N. Bezmaternykh, A. D. Vasil'ev, *et al.*, J. Magn. Magn. Mater. **272**–**276**, E359 (2004).
9. A. I. Pankrats, G. A. Petrakovskiĭ, L. N. Bezmaternykh, and O. A. Bayukov, Zh. Éksp. Teor. Fiz. **126**, 887 (2004) [JETP **99**, 766 (2004)].
10. A. K. Zvezdin, V. M. Matveev, A. A. Mukhin, and A. I. Popkov, *Rare-Earth Ions in the Magnetic Ordered Crystals* (Nauka, Moscow, 1985) [in Russian].
11. R. Z. Levitin, E. N. Popova, R. M. Chtsherbov, *et al.*, Pis'ma Zh. Éksp. Teor. Fiz. **79**, 531 (2004) [JETP Lett. **79**, 423 (2004)].
12. A. G. Gavrilyuk, S. A. Kharlamova, I. S. Lyubutin, *et al.*, Pis'ma Zh. Éksp. Teor. Fiz. **80**, 482 (2004) [JETP Lett. **80**, 426 (2004)].
13. N. N. Greenwood and T. C. Gibb, *Mössbauer Spectroscopy* (Chapman and Hall, London, 1978).